~~ORIGINAL~~
12/9/97

MICROSTIMULATORS AND MICROTRANSDUCERS FOR FUNCTIONAL NEUROMUSCULAR STIMULATION

Contract #N01-NS-5-2325
Quarterly Progress Report #10 -
Period: June 10, 1996 - September 9, 1997

ALFRED E. MANN FOUNDATION FOR SCIENTIFIC RESEARCH
12744 San Fernando Road, Sylmar, CA 91342
Joseph H. Schulman, Ph.D., Principal Investigator
John Gord, David Fencil, David Payne, Cecilia Tanacs, Larry Devor
Irma Vasquez-Jiminez, Yolanda Covarrubias, Joseph Walker

BIO-MEDICAL ENGINEERING UNIT, QUEEN'S UNIVERSITY
Kingston, ON K7L 3N6 CANADA
Frances J.R. Richmond, Ph.D., Principal Investigator
Gerald Loeb, Kevin Hood, Ray Peck, Anne Dupont, Tiina Liinamaa

PRITZKER INSTITUTE OF MEDICAL ENGINEERING, ILLINOIS INSTITUTE OF TECHNOLOGY
Philip R. Troyk, Ph.D., Principal Investigator

THIS QPR IS BEING SENT TO YOU BEFORE IT HAS BEEN REVIEWED BY THE STAFF OF THE NEURAL PROSTHESIS PROGRAM.

ABSTRACT

We are developing a new class of implantable electronic devices for a wide range of neural prosthetic applications. Each implant consists of a microminiature capsule that can be injected into any desired location through a 12 gauge hypodermic needle. Multiple implants receive power and digitally-encoded command signals from an RF field established by a single external coil. The first two types of implant that we have made were single-channel microstimulators equipped with either a capacitor-electrode or an internal capacitor that stores charge electrolytically and releases it upon command as current-regulated stimulation pulses. We are also working on implants equipped with bidirectional telemetry that can be used to record sensory feedback or motor command signals and transmit them to the external control system.

In this quarter, we continued accelerated life-testing of various batches of BION implants, all of which were built without the water-getter insert. Continuing concern about the nature and robustness of the glass-to-PtIr seal led us to study the feasibility of using tantalum tubes for the iridium electrode end, in the hope of employing a seal similar to the more reliable glass-to-Ta-stem seal at the tantalum electrode end. We demonstrated that the presence of tantalum connected to the iridium electrode and exposed to saline was electrochemically stable during active use of the device at its maximal rated output.

The histological results from the first set of passive devices implanted for long-term animal studies demonstrated that BIONs cause histological reactions that are less than or equal to negative control materials typically used for such studies. The remaining two scientific articles

from our previous series of active BION tests in animals were accepted for publication in IEEE-BME (Cameron et al., in press a & b).

Also in this quarter we discovered several layout flaws in the new ASIC chip that affected several improvements including the increased compliance voltage of 18 volts.

The corrections were made and resubmitted on additional MOSIS runs. This work was performed jointly between the Mann Foundation and Pritzker by John Gord and Philip Troyk.

During this quarter we tightened up the traceability and documentation of BION prototype production units.

IMPLANTABLE DEVICES

Accelerated life-test results at Queen's

The chronic test chamber described in the last QPR has been functioning well for the past quarter at Queen's University and a duplicate system was built and sent AEMF for similar testing there. The chamber includes 8 individual polypropylene chambers with recording electrodes that permit BIONs to be soaked in saline, continuously temperature cycled (3 hours @ 37C and 9 hours @ 77C), continuously stimulated at maximal rated output (10 mA x 258 us @ 50 pps), and monitored for output pulse parameters at hourly intervals.

Figure 1 shows the sort of continuous plot generated for a device that is working properly (A006) and a device that is failing in the typical manner as a result of a slow leak of water vapor into the glass capsule (A191). Properly functioning devices tend to produce lower output currents at higher temperatures because of ASIC properties. Occasional drop-outs are due to air bubbles around their electrodes; bubbles are easily removed by opening the screw-top on the chamber and reseating the assembly holding the BION and recording electrodes. These bubbles

are room air that leaks into the chambers and accumulates during temperature cycling, rather than electrolysis products at the electrodes. Defects in the hermetic seals result in accumulation of water vapor inside the BION glass capsule. This water vapor tends to condense at the lower temperatures and revaporize at the higher temperatures. When water vapor condenses on the tuned RF receiving coil, its high dielectric constant (80 vs. 1 for air) lowers the resonant frequency of the coil, resulting in dropouts of device function. The pattern of intermittent function illustrated for device A191 was always associated with visible water condensation in the glass capsule when cooled to room temperature and examined under a dissecting microscope.

Figure 2 shows the results to date for chronic testing of samples from four batches of device fabrication. The vertical dashed lines show the elapsed test time at which the device would have experienced the equivalent of a 10 year life under normal use circumstances. It takes about 1 month for these maximally activated devices to accumulate the total stimulation charge output normally expected for 10 years of clinical TES. A slow leak of moisture that in two months reaches 100% humidity at 37C in these devices (without water getters) would normally not reach saturation for 10 years with the water getter evaluated in our previous QPR. General thermodynamic aging of various materials following an Arrhenius temperature dependency would experience the equivalent of 10 years of life at 37C in about 3 months at 85C (our original test temperature) or 5 months at 77C (the temperature now in use). Nevertheless, except for the three devices still running or terminated electively, none of these results is acceptable to us. Almost all of the failures are related to moisture leaks and these leaks appear to be worse in the most recent batches.

The failed devices and others from these batches have been reexamined for leaks using

the new bomb-bubble-tester described in the previous QPR.

Three of the recent devices have slow leaks from the final metal-to-metal seal. which now consists of a Pt ball swaged into the end of the PtIr tube and melted in place with the YAG laser (see Fig. 3). While such seals are fairly routine in the industry, this particular version has not been shown to work in this application. The new tester has revealed leaks both at the end of the tube and in the Pt-Ir tube under the Ir electrode. Various changes are underway, including those related to the possible change to a Ta tube as described below.

The remaining leaks were between the glass bead and the PtIr tube, which is more problematic. These were slow leaks, in the range 10-9 to 10-10 cc He atm/s, which were measurable in the Alcatel helium leak detector but which produced no visible bubbles in the bomb-bubble tester. All of these leaks were associated with low compression of the glass bead on the PtIr stem, as revealed by photoelastic stress measurements. We are in the process of determining why this photoclastic stress is less than that observed on non-leaking units. We have also found that there was poor control of the beam power in the CO2 laser used to melt the glass bead onto the PtIr tube. The laser was cooled by a recirculating water bath with a 5 gallon reservoir. This was sufficient in the early days of the project when the laser was only operated for an hour or so at a time. Recently, we have been running the laser almost continuously for the entire day, producing stocks of subassemblies for development and validation of assembly procedures. After encountering these sealing problems, we tracked the power output of the laser and the temperature of the reservoir and found them to be negatively correlated. By the end of the day, the water tended to increase from 21C to 36C and the laser power dropped by 30%, a large value compared to the known tolerance window for producing acceptable PtIr-glass seals.

This problem has now been corrected by installing a thermostatically controlled water chiller, and incidentally increasing the flow rate through the laser.

PROPOSED TANTALUM TUBE CONSTRUCTION

At best, the PtIr-glass seals are theoretically and empirically more problematic than the Ta-glass seals. The Kimbel N51A borosilicate glass that we use has a much better match to tantalum than to 90% platinum-10% iridium for coefficient of thermal expansion. Ta-glass seals that are hermetic tend to have relatively little residual stress in the glass when measured by photoelastic stress. PtIr-glass seals have a relatively narrow and much higher window of acceptable stress levels; below this they consistently produce slow leaks (of the sort revealed during chronic soak testing) and above this they tend to fracture spontaneously when placed in a polar solvent such as water. Tantalum tends spontaneously to have a more predictable and stable surface oxide than PtIr, which promotes bonding of the glass to the metal without requiring mechanical compression. Empirically, we have had very little difficulty obtaining high yields of hermetic Ta-glass seals and almost no failures of completed devices attributable to that seal.

The above circumstances led us to consider the possibility of using Ta for the tubular feedthrough. The electrochemical implications of this are considered in the next section. Figure 1 shows a proposed revision to the implant assembly sequence that would incorporate a Ta tube along with several concurrent design changes under development. In particular, the non-noble nature of the Ta tube requires a positive weld between the spring and the tube rather than the mechanical butt-joint that was originally proposed for the PtIr tube. This led us to specify a Ta tube small enough to fit inside the elgiloy spring to facilitate a lateral resistance weld. We have located a supplier for various sizes of Ta tubes and components have been ordered. We hope that

smaller and/or thicker walled tubes can beYAG-welded shut without a plug, eliminating that component and step and facilitating vacuum bake-out, which is compromised in the present design shown in Figure 3. Further, it may be possible to join the Ir electrode to the Ta tube in the same step as sealing the tube. This was not possible with the 0.020" PtIr tube because it required too much energy and that energy tended to be conveyed by thermal conduction to the already stressed glass-PtIr seal, causing fractures. Note that the design in Figure 4 eliminates two components (PtIr washer and Pt plug), eliminates two YAG welds (adding one resistance weld), eliminates handling of a loose spring during final assembly, and maximizes getter volume.

TANTALUM-IRIDIUM ELECTRODE TESTING

The electrochemical interactions between the Ta capacitor electrode, the activated-Ir counterelectrode and the unique power storage scheme of the BION were developed and tested in the early days of this project and have not been reconsidered since (Loeb et al., 1991). Based on work at EIC laboratories, it was known that mixed electrode surfaces containing both activated Ir and other noble metals such as Pt had electrochemical properties that were dominated by the activated Ir. There does not seem to be any experience with a mixed surface of Ir and Ta such as would occur with a Ta tubular feedthrough attached to an Ir counter-electrode in the BION. Therefore, we devised a test in which we chronically stimulated BIONs having a Ta-Ir counterelectrode and looked for dissolved tantalum in the surrounding saline and for signs of corrosion on the electrodes in the scanning electron microscope.

We constructed three BION implants using the usual Ir electrode on a Pt-Ir tube but with an added YAG-welded piece of Ta wire attached to the Ir surface. These devices plus an additional control BION with only the usual electrode materials were examined in the SEM. We

photographed details of the grain structure around relocatable surface features such as scratches and weld seams, which are also sites that might tend to concentrate the effects of any corrosion. A total of 10 devices (the 3 Ta-Ir test units plus 7 controls) were stimulated continuously in saline in our temperature-cycling chronic test unit for periods of 18 to 56 days. Approximately 1 cc of phosphate-buffered isotonic saline was contained in each polypropylene test chamber; this was not changed throughout the course of the chronic testing, topping up only as needed with distilled water to replace evaporative loss as necessary. The 10 saline samples plus two samples of saline from test chambers that contained no BIONs were sent to Analytical Services Laboratories. Ltd., Vancouver, BC, for quantitative assay of dissolved tantalum by atomic absorption spectrophotometry. All of these samples had no detectable tantalum at the limit of resolution of the test method (<0.010 mg/l = 10 ppb) except for one of the control BION samples, which was reported as detectable at the limit of resolution (.010 mg/l).

Figure 5 shows before-and-after comparisons of typical sites on the Ta-Ir test electrodes. No significant changes in grain structure were noted at any sites on the Ta-Ir or control BIONs. One new feature was noted visually on one Ta-Ir test unit only - a small amount of powdery, light green residue attached to the PtIr stem just as it exited from the glass bead (not shown). This turned out to be nickel chloride according to EDS scanning, which we presume to be a contaminant from the Dumont nickel-alloy forceps used to shape the Ir recording electrodes in the test chambers. The presence of this deposit actually confirms that the Ir counterelectrode tends to have a small cathodal bias, as would be expected as a result of the continuous anodal charging of the Ta capacitor electrode. This cathodal bias would tend to protect any non-noble exposed metal from oxidation and corrosion, as well as plating out any metallic contaminants

that might already be in solution. We were concerned that the intermittent anodal excursions of the Ir electrode associated with output pulses might cause corrosion of the tantalum once it was stripped of its normal oxide surface by such cathodal polarization. Replating of Ta between pulses would account for the absence of Ta in solution, but such replating would be associated with amorphous deposits such as the nickel deposit actually detected. No such Ta deposits were detected nor were there any signs of loss or replating of Ta at crystal grain boundaries or seams with other metals.

CHRONIC PASSIVE ANIMAL TESTING

As part of the standard preclinical testing required for Class III medical devices, we are studying the nature of the histological reaction that occurs in muscle tissue surrounding passive BIONs at intervals of 1, 3, 6 and 12 months in cats. This complements the previous study of active BIONs (Cameron et al., in press b), which employed implants with the same electrode materials but an earlier package design using different electrode shapes and different hermetic sealing processes (Cameron et al., 1997). Figure 6 shows the results for 1 month implants of the new BION design (non-coated BION), compared to a variation in which a thin-walled sleeve of silicone elastomer is shrunk over the glass capsule leaving only the electrodes exposed, silicone tubes with dimensions similar to a BION, and a standard negative control rod for biocompatibility testing made from USP-approved polyethylene. Six wet muscle samples from each cat (3 cats; total of 18 samples) were sent to CVD, Inc. (West Sacramento, CA 95691). The tissue was processed, blocked, sectioned, and stained with H&E and examined microscopically. Implant sites were graded for standard changes using a grading system where 0=no change, 1=minimal, 2=mild, 3=moderate and 4=severe. In addition, the width of the reactive capsule was

measured in microns. Inflammatory changes were qualitatively similar in all sites from all three cats. but quantitatively varied as to various components. The cell scores and capsule thicknesses for all implants indicate no increased inflammatory reactions over negative controls. It is interesting to note that the BIONs tended to produce slightly less reaction than the controls, particularly when coated with silicone. This may be due to the tissue anchoring afforded by the necks of the electrodes at either end, which probably reduces abrasion of the capsular tissue against the implant surface as the surrounding muscle moves actively and passively.

ASIC DEVELOPMENT

Progress Report for Work at the Pritzker Institute

During the last quarter, work at the Pritzker Institute has focused upon analysis of the MOSIS integrated circuits.

Integrated Circuit Layout Revisions

Previously we had reported about the efforts leading to the submission of the revised 2 MHZ microstimulator and the Repeater Chip to MOSIS for fabrication at AMI. The revision of these layouts was accomplished by a coordinated effort between IIT and Slicex. Verification of the design rules was accomplished at Slicex, and layout-vs.-schematic verification was performed at IIT. The microstimulator chip and the Repeater chip saw extensive layout revisions. In addition, a "test chip" was also submitted which contained various portions of the Repeater chip circuitry.

Prior to delivery of the chips it was discovered that an unfortunate error existed in the layout at the upper-most cell level. A long strip of via/contact had been placed, by Slicex, across

the entire length of the Repeater chip, rendering it inoperative. Equally unfortunate was the substitution of cells from an earlier revision of the layouts in the test chip. Therefore neither of these chips were functional upon delivery.

Fortunately, some of the circuits used in the Repeater chip design had been included in another MOSIS submission as part of work on IIT's contract: Multichannel Transcutaneous Cortical Stimulation System. Therefore we were able to use that chip, MOS2, to test the power supply regulator, and rectifier/data decoder. Both of these circuits are key components for the telemetry of the proposed micromodules.

Testing of MOSIS Integrated Circuits

The chip, MOS1, was used to examine the operation of the voltage regulator and the power rectifier/data decoder. The regulator performed as expected from the simulation results. The rectifier circuit was seen to have a two-transistor parasitic which interfered with its normal operation. By way of review, we include the block diagram for the Repeater chip, below. The portions of the diagram labeled "full wave rectifier" and "data sensor" and "housekeeping circuit" were included on MOS1. These circuits rectify the coil voltage to provide a D.C. power supply, decode suspended carrier incoming data, and provide low-voltage regulated power supplies for the logic and voltage references, respectively.

Repeater Chip Block Diagram

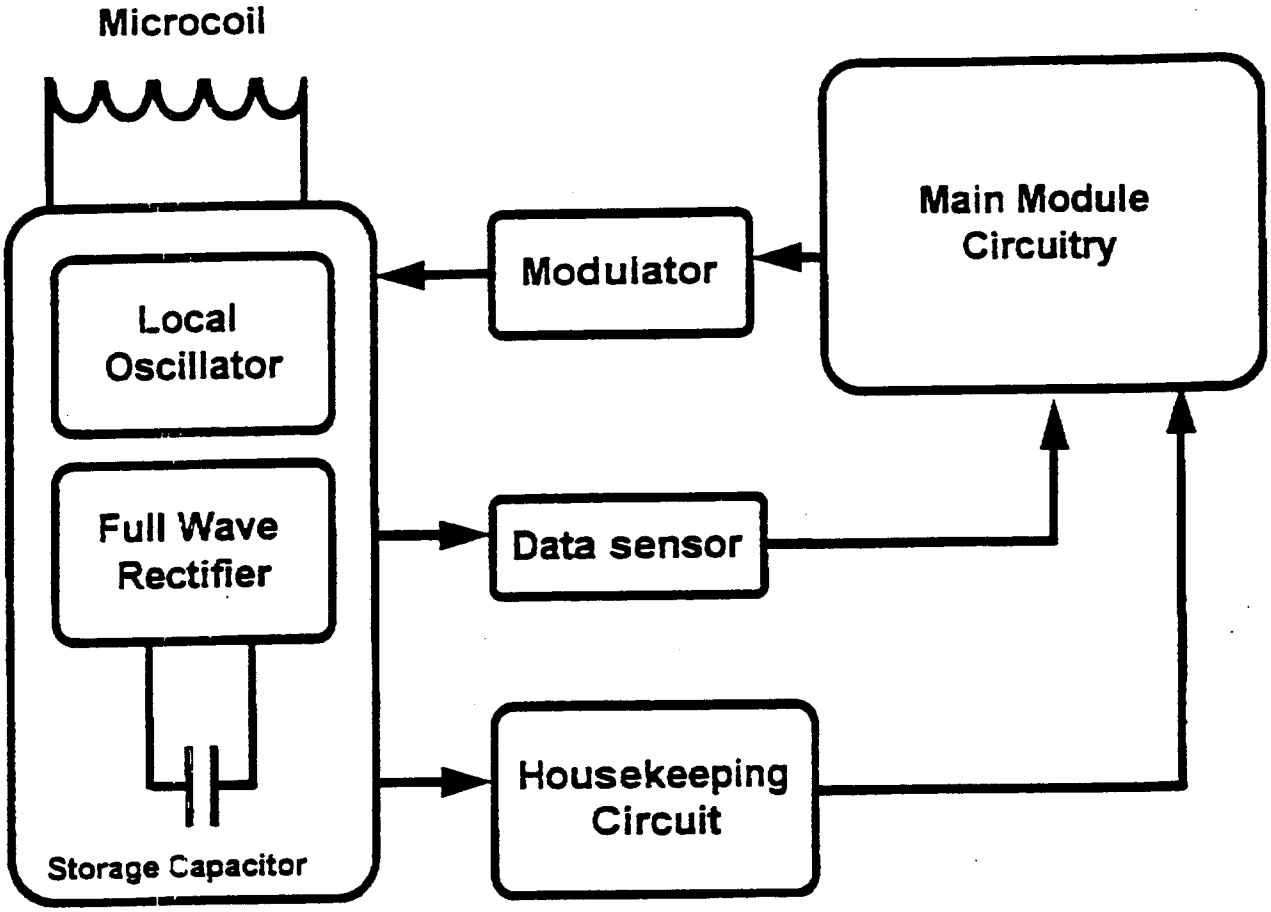

The parasitic structure, identified in the full wave rectifier, was composed of a horizontal NPN and a vertical PNP transistor. The basic configuration of the parasitic is shown below:

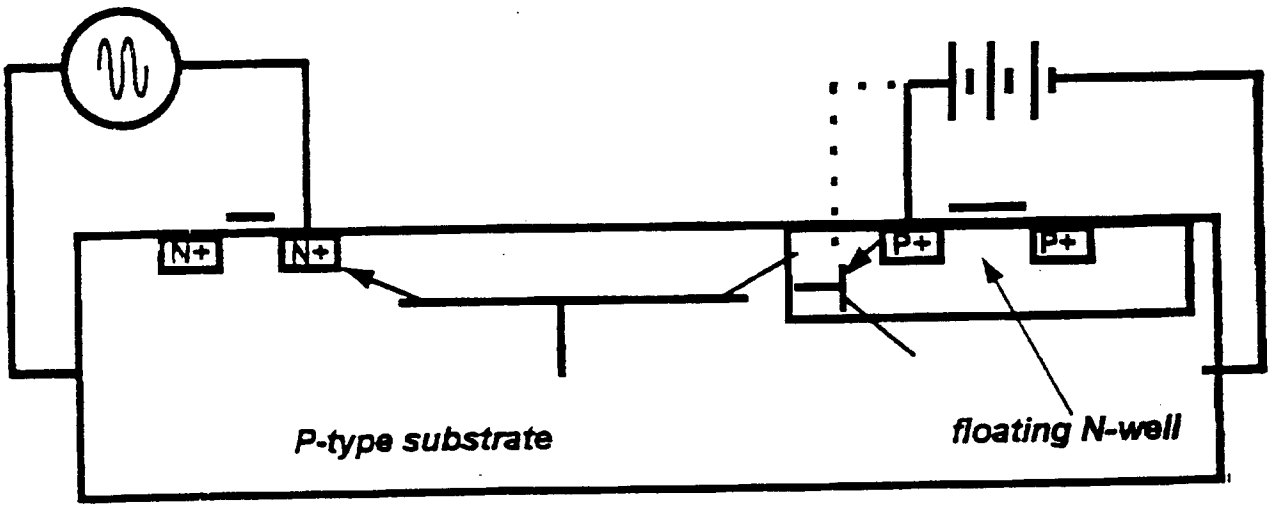

The problem is caused by the need for the floating N-well, which contains the upper bridge P-channel fets. The floating well is required to prevent the vertical PNP transistor from turning on when the sources of the P-fets exceed the power supply rail. We had analyzed this problem in design and layout. The proposed solution was the large spacing between the N-channel lower rectifiers and the floating well. A distance of over 50 microns was allowed, and it was felt that this distance would be large enough to prevent substrate-injected carriers from reaching the floating well.

Unfortunately, this was not the case. Although the beta of the horizontal transistor was less than 1, the vertical transistor had sufficient gain, about 80, to cause an unacceptable current to flow from the power supply rail to the chip substrate via the vertical transistor. We speculate that improvements in the purity of silicon wafers have contributed to longer carrier lifetimes, and consequently less immunity to horizontal parasitic bipolars, regardless of the width of the base region. For testing purposes, we were able to shunt the lower N-fets with shotkey diodes, thus preventing the horizontal transistors from conducting.

In a future chip fabrication we intend to use the guard-bar structure depicted below:

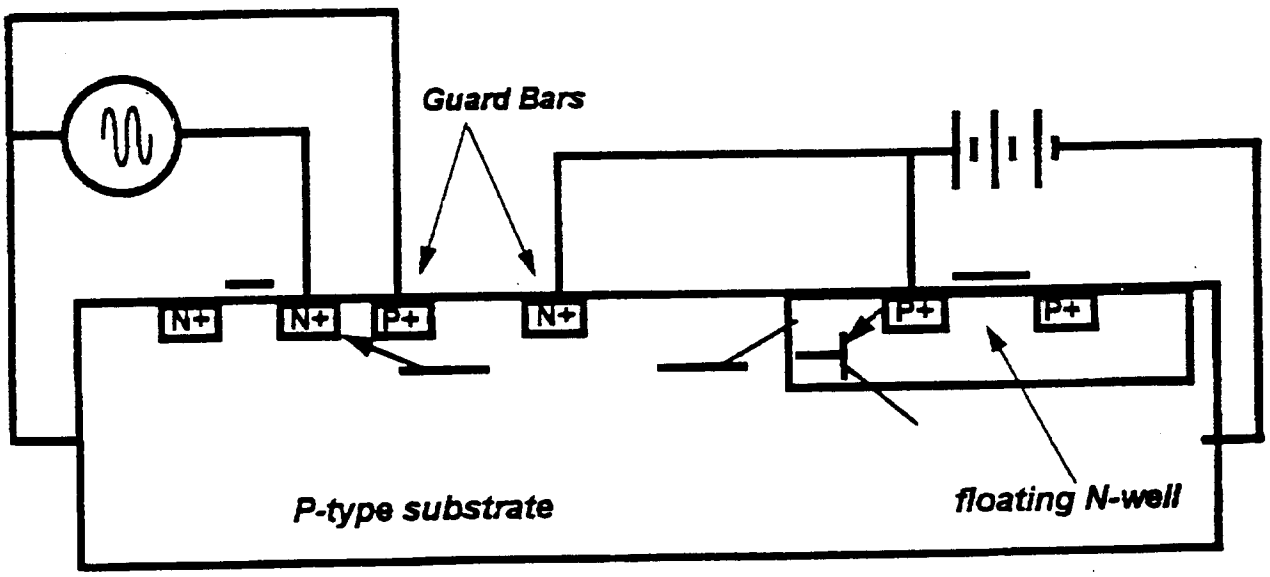

We feel that several pairs of these guard bars will prevent the N-fet substrate-injected current from becoming horizontal-transistor base current.

Using the shunt diodes for test purposes, we were able to proceed with the examination of the data sensor, when the transmitter was modulated using the suspended-carrier scheme. By way of review the following diagram shows the method of demodulation employed by this circuit:

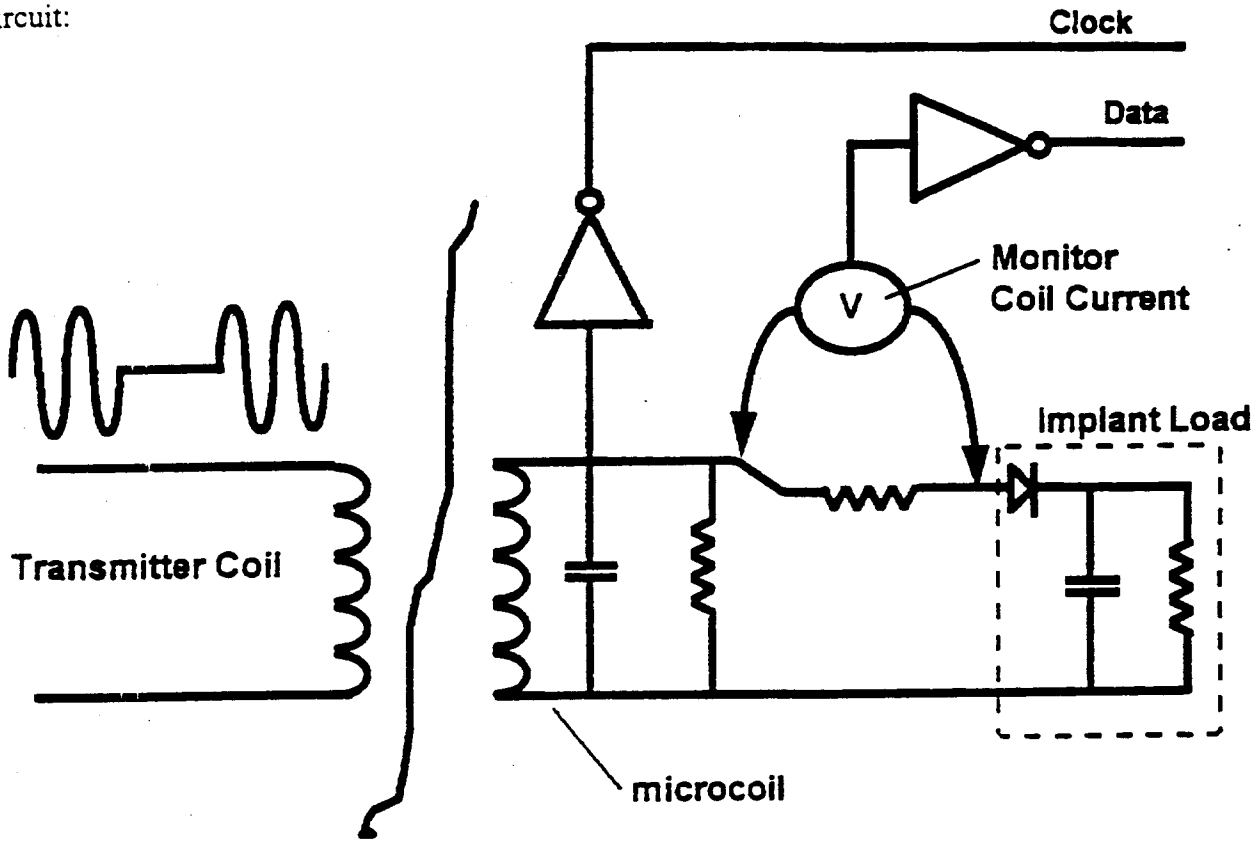

This diagram is pictoral, only, and does not precisely show the method used to sense the rectifier currents.

We were able to test two functions of the data sensor: clock recovery and data demodulation. In the oscilloscope photo below, the clock recovery during 2-cycle-on-2-cycle-off transmitter modulation can be seen. The lower trace shows the coil current at 1-amp/division,

and the upper trace shows the digital clock output at 1-volt/division. Note that the clock recovery continues even during the 2 cycles in which the transmitter is turned off.

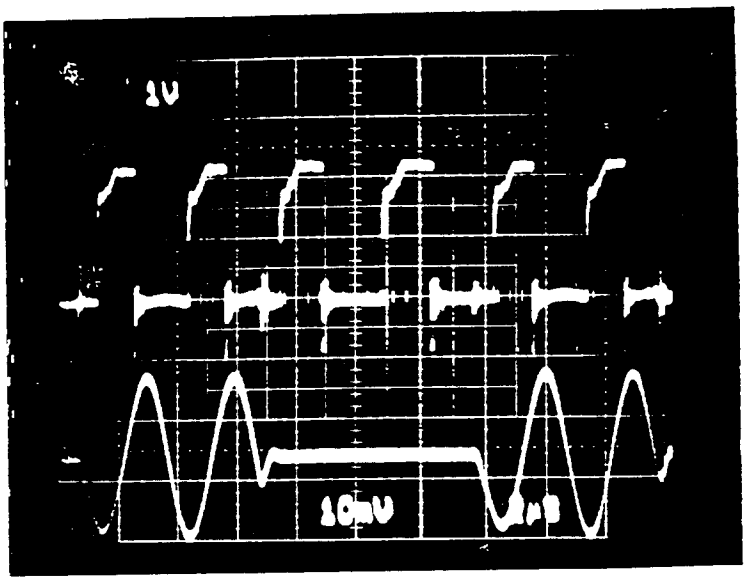

In the oscilloscope photo, below, the output of the data sensor is shown. The lower trace shows the coil current and the upper trace shows the digital demodulated data output. Note that one pulse can be seen for each of the periods during which the transmitter is turned off.

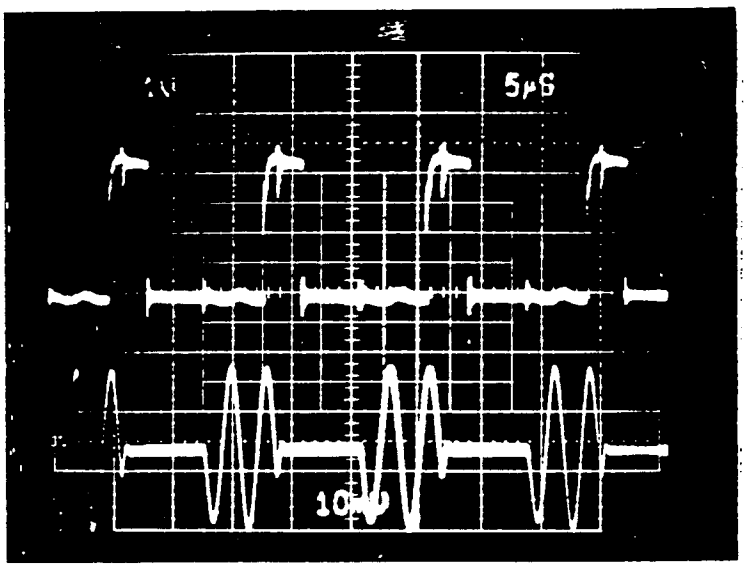

Transmitter Fabrication and Delivery

Although the appropriate excitation and modulation parameters for the new AMI 2MHz microstimulator is not presently known, we have continued to support device testing taking place at Queen's University. New transmitter coils have been wound, at Queen's, and we are presently attempting to fit them to transmitters.

Next Quarter

A new concept for an improved case and hermetic seal that is easy to manufacture and more reliable has been suggested. This will be described in the next quarterly progress report.

References

Loeb, G.E., Zamin, C.J., Schulman, J.H. and Troyk, P.R. Injectable microstimulator for functional electrical stimulation. Med. & Biol. Engng. and Comput. 29:NS13-NS19, 1991.

Cameron, T., Loeb, G.E., Peck, R.A., Schulman, J.H., Strojnik, P. and Troyk, P.R. Micromodular implants to provide electrical stimulation of paralyzed muscles and limbs. IEEE Trans. Biomed. Engng., 44:781-790, 1997.

Cameron, T, FJR Richmond and GE Loeb. Effects of regional stimulation using a miniature stimulator implanted in feline posterior biceps femoris. IEEE Trans. Biomed. Engng., in press a.

Cameron, T, TL Liinamaa, GE Loeb and FJR Richmond. Long-term biocompatibility of a miniature stimulator implanted in feline hind limb muscles. IEEE Trans. Biomed. Engng., in press b.

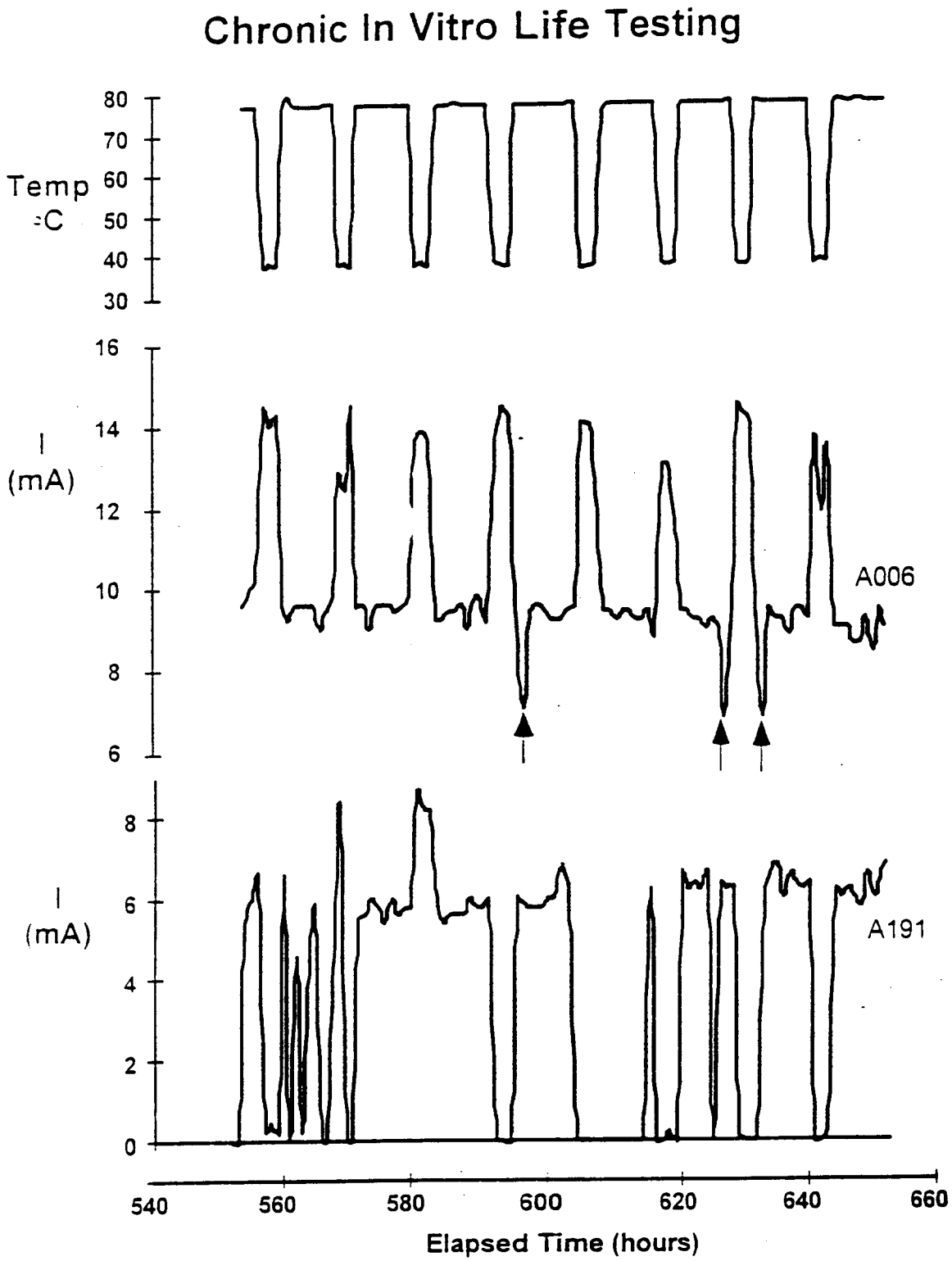

Figure 1: Typical chronic test results during temperature cycling with continuous maximal rated output: hourly measures of output current plotted here for BION serial numbers A006 and A191. Device A006 was functioning normally, with output current decreasing at higher temperatures; occasional drops in output current (arrows) were due to air bubbles around the recording electrodes. Device A191 was failing due to moisture in the capsule. It tended to function only at the higher temperatures and then intermittently. At the lower temperatures, water condensation on the receiving coil shifted its resonant frequency so that it was no longer responsive to commands.

BION Chronic Testing:

10 Year Life Criteria Based on Acceleration

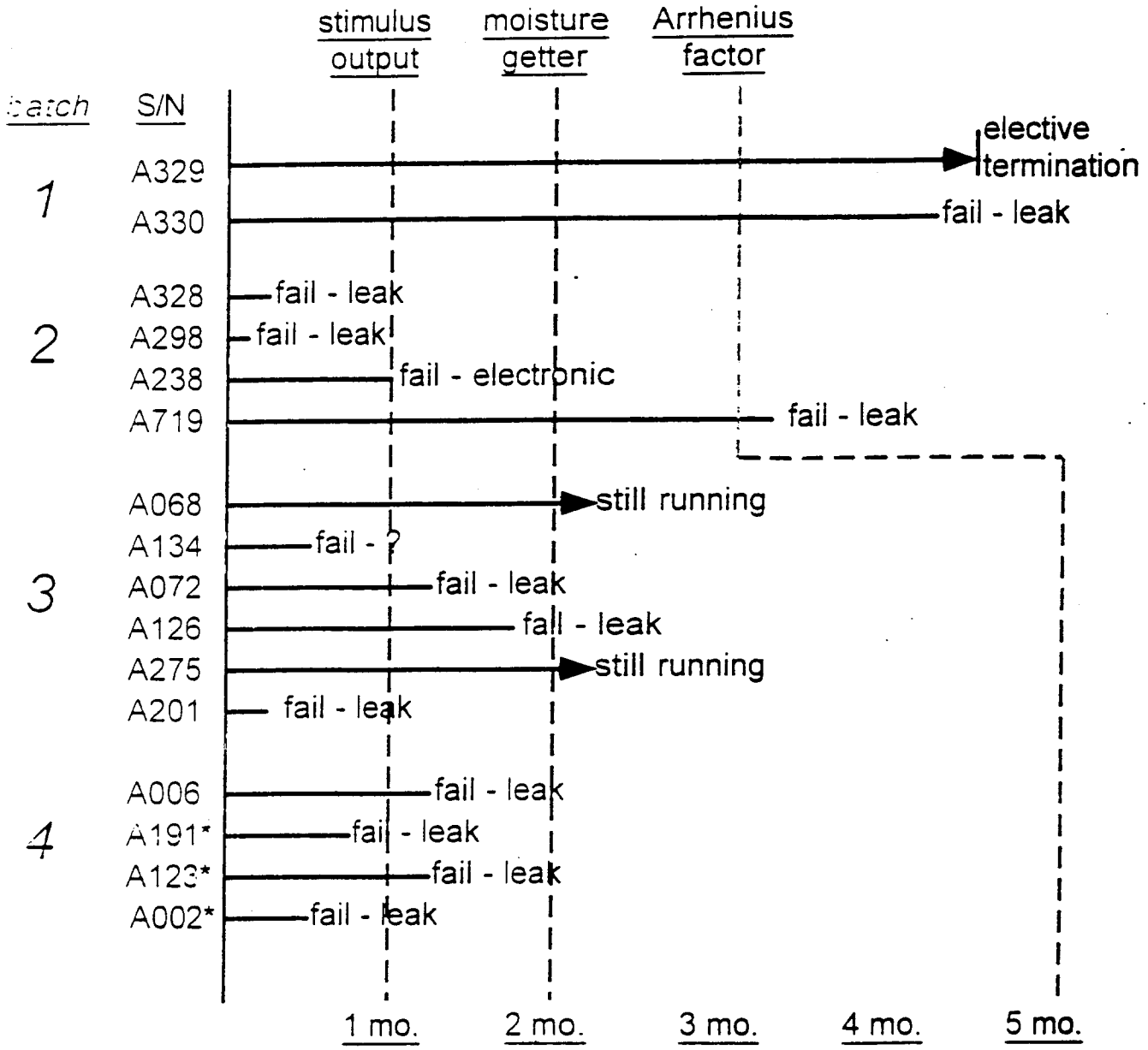

Fig. 2

BION™ Implant Assembly Sequence

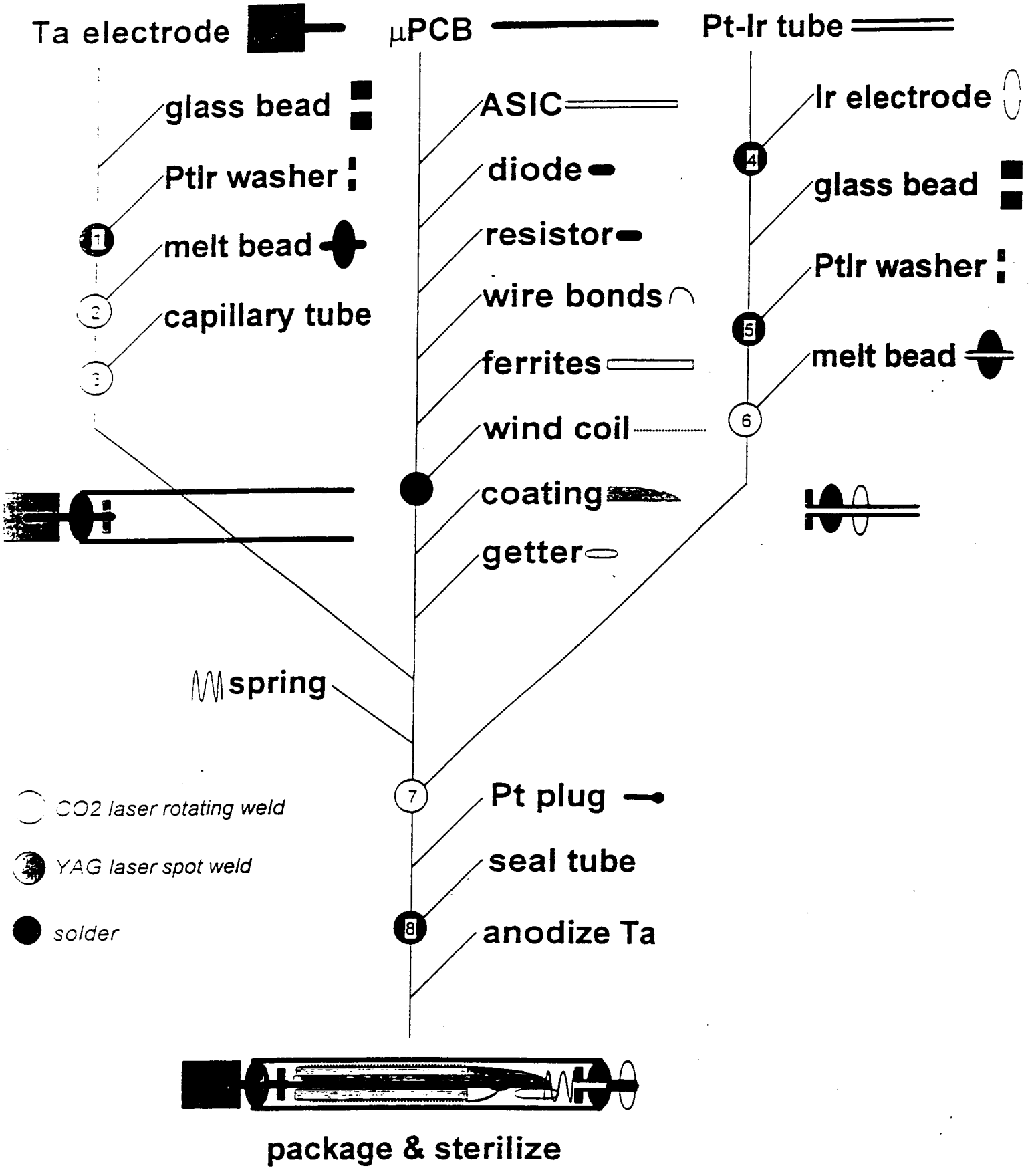

BION™ Implant Assembly Sequence (revised)

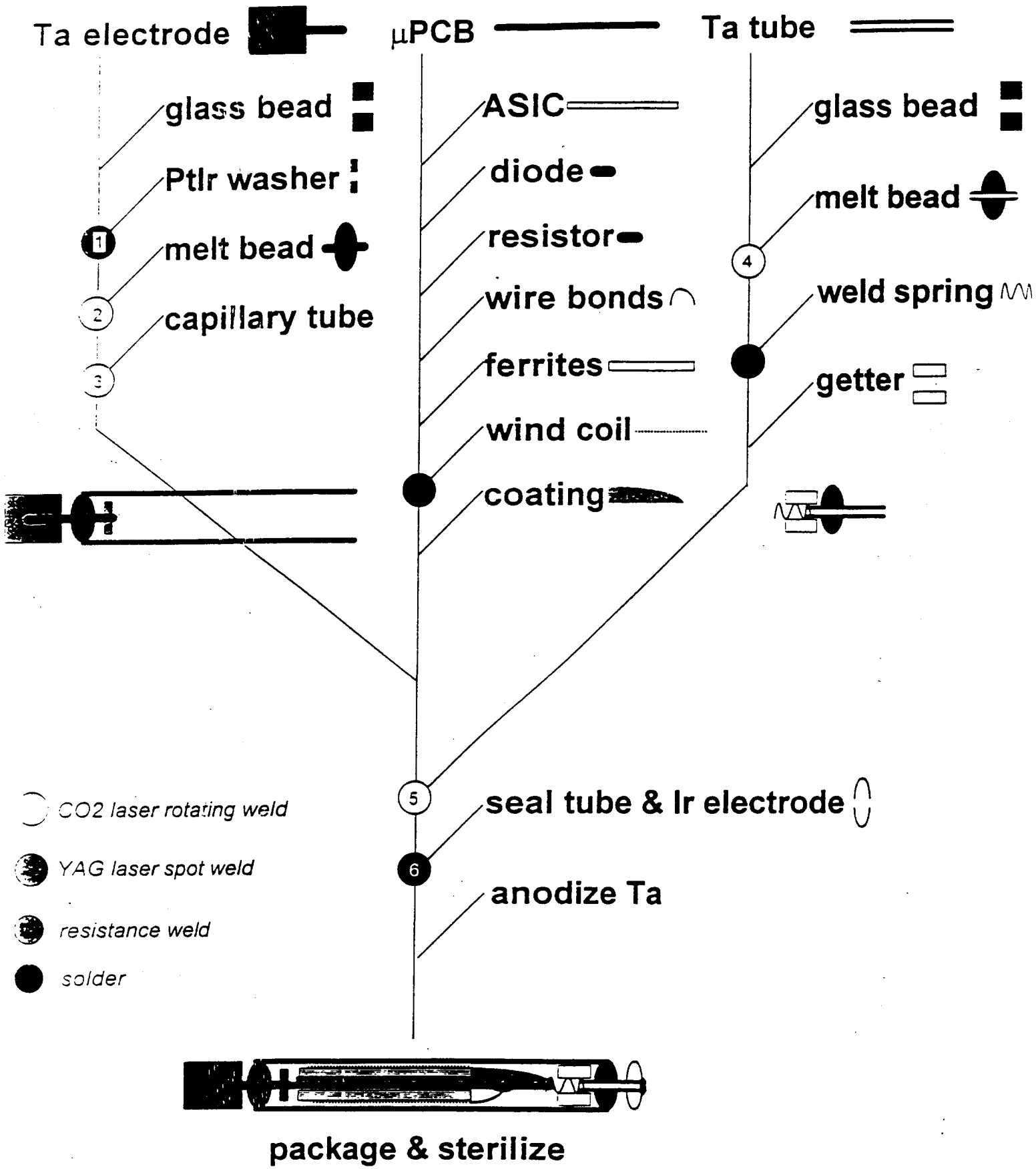

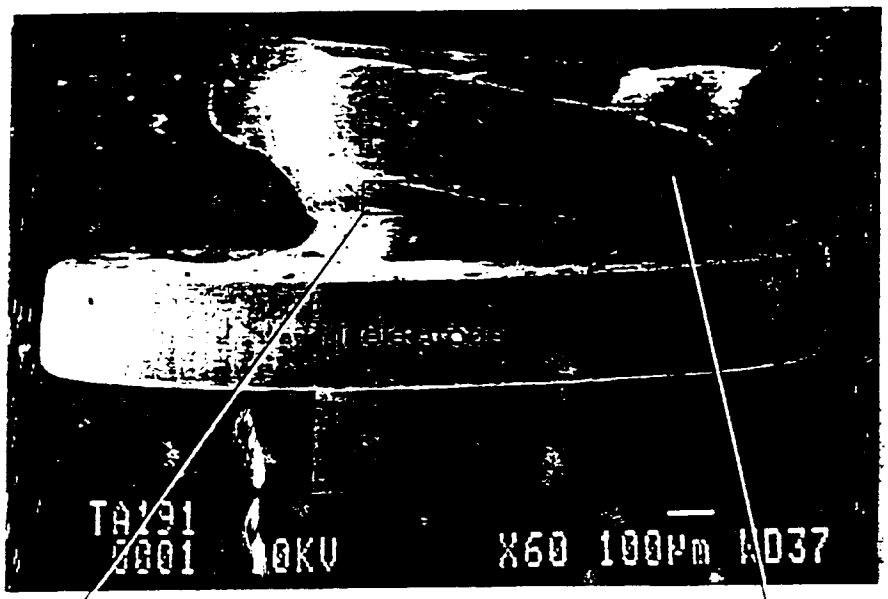

YAG melt

Ta wire - Pt plug

Ta wire

Before Stimulation

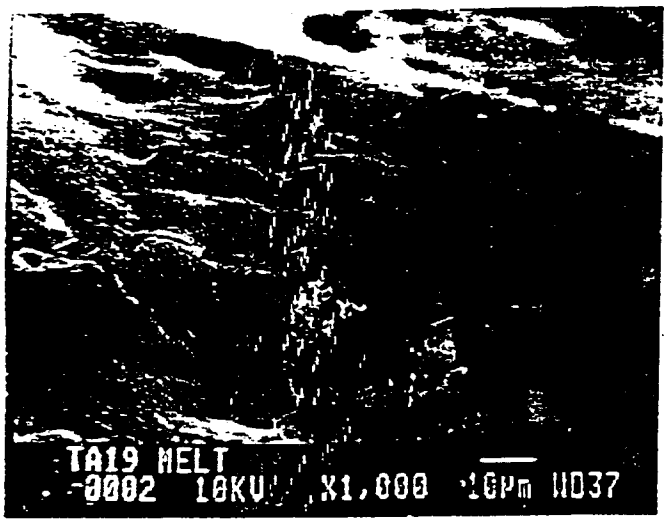

After 28 Days Stimulation

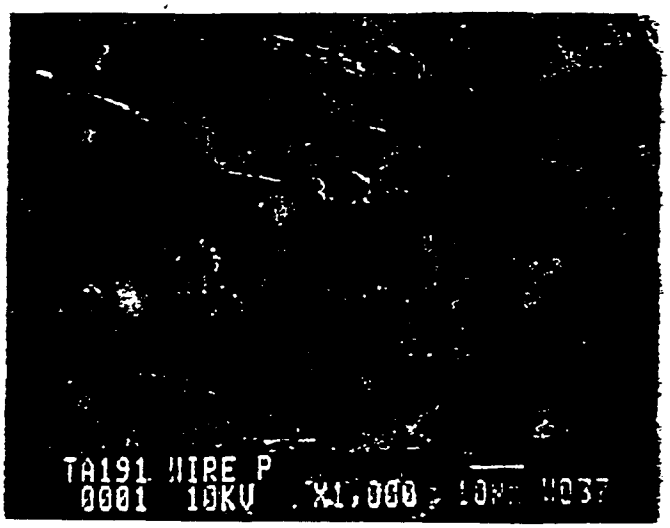

Cell Scores and Capsule Thicknesses For 1 Month Implant Cats